Do ridge–ridge–fault triple junctions exist on Earth? Evidence from the Aden–Owen–Carlsberg junction in the NW Indian Ocean

M. Fournier,*† C. Petit,† N. Chamot-Rooke,* O. Fabbri,‡ P. Huchon,† B. Maillot§ and C. Lepvrier†

*Laboratoire de Géologie, CNRS, Ecole Normale Supérieure, Paris, France
†Laboratoire de Tectonique, CNRS, Université Pierre et Marie Curie-Paris 6, UCP, Paris, France
‡ Département de Géosciences, Université de Franche-Comté, Besançon, France
§ Laboratoire de Tectonique, CNRS, Université de Cergy-Pontoise, UPMC, Cergy-Pontoise

ABSTRACT

The triple junctions predicted to be ridge–ridge–fault (RRF) types on the basis of large-scale plate motions are the Azores triple junction between the Gloria Fault and the Mid-Atlantic Ridge, the Juan Fernandez triple junction between the Chile Transform and the East Pacific Rise and the Aden–Owen–Carlsberg (AOC) triple junction between the Owen fracture zone (OFZ) and the Carlsberg and Sheba ridges. In the first two cases, the expected RRF triple junction does not exist because the transform fault arm of the triple junction has evolved into a divergent boundary before connecting to the ridges. Here, we report the results of a marine geophysical survey of the AOC triple junction, which took place in 2006 aboard the *R/V Beautemps-Beaupré*. We show that a rift basin currently forms at the southern end of the OFZ, indicating that a divergent plate boundary between Arabia and India is developing at the triple junction. The connection of this boundary with the Carlsberg and Sheba ridges is not clearly delineated and the triple junction presently corresponds to a widespread zone of distributed deformation. The AOC triple junction appears to be in a transient stage between a former triple junction of the ridge–fault–fault type and a future triple junction of the ridge–ridge–ridge (RRR) type. Consequently, the known three examples of potential RRF triple junctions are actually of the RRR type, and RRF triple junctions do not presently exist on Earth.

INTRODUCTION

Soon after the advent of plate tectonics, researchers have noticed that there should be points where three plates and their boundaries meet. McKenzie & Morgan (1969) explored the potential stability of such triple junctions by predicting the evolutionary behaviour of plate boundaries at the local scale based on the large-scale motions of the plates. The velocity–space representation of local velocities that they developed is still extremely useful in studying these junctions, although almost nowhere can the triple junction evolution be predicted using their assumptions. Part of the problem lies in the assumption that oceanic ridges should spread symmetrically and orthogonally to the ridge axis. Even at relatively simple triple junctions, such as the ridge–ridge–ridge (RRR) Rodriguez triple junction in the Indian Ocean, the ridges do not spread orthogonally (Tapscott *et al.*, 1980; Munschy & Schlich, 1989; Patriat & Parson, 1989; Mitchell, 1991; Mitchell & Par-

son, 1993; Honsho *et al.*, 1996). Another problem with the velocity–space diagram analysis has been that the type of plate boundary at triple junctions is not predictable only from the large-scale plate motions. In the Pacific, the Galapagos and Juan Fernandez junctions have both turned out to contain microplates (Lonsdale, 1988; Larson *et al.*, 1992; Bird & Naar, 1994; Bird *et al.*, 1998; Klein *et al.*, 2005), and in the Atlantic, the Azores and Bouvet junctions correspond to zones of distributed deformation where the three-plate boundaries do not meet at a point (Sclater *et al.*, 1976; Searle, 1980; Luis *et al.*, 1994; Ligi *et al.*, 1997, 1999; Mitchell & Livermore, 1998; Fernandes *et al.*, 2006). Here, we investigate the potential stability of ridge–ridge–fault (RRF) triple junctions where one transform fault meets two spreading ridges.

In the oceanic domain, three active examples of RRF triple junctions are known on Earth (Fig. 1): (1) the Azores triple junction in the Atlantic Ocean, which connects the Gloria transform fault and the Mid-Atlantic Ridge (Searle, 1980; Argus *et al.*, 1989), (2) the Juan Fernandez triple junction in the Pacific Ocean, which connects the Chile Transform and the East Pacific Rise (Larson *et al.*, 1992), and (3) the Aden–Owen–Carslberg (AOC) triple junction

Correspondence: Marc Fournier, Laboratoire de Géologie, CNRS, Ecole Normale Supérieure, 24 rue Lhomond, 75005 Paris, France. E-mail: marc.fournier@upmc.fr
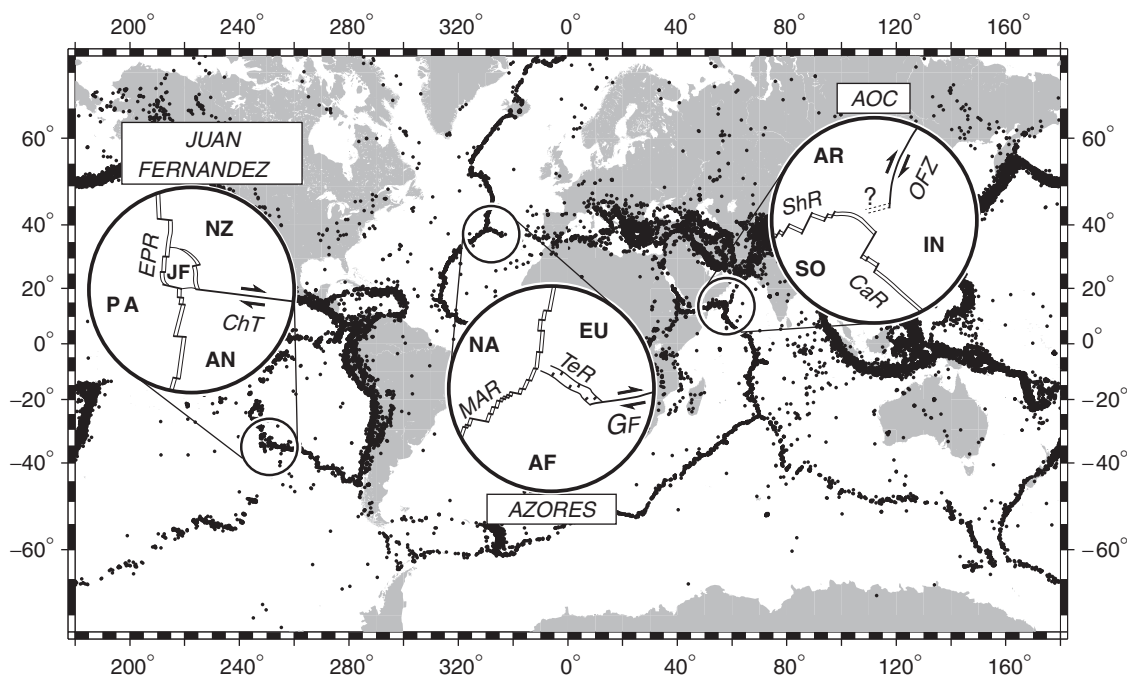
Fig. 1. Location of the three active examples of connection of a transform fault with two spreading ridges on Earth: the Gloria Fault (GF) with the Mid-Atlantic Ridge (MAR) at the Azores triple junction, the Chile Transform (ChT) with the East Pacific Rise (EPR) at the Juan Fernandez triple junction, and the Owen fracture zone (OFZ) with the Carlsberg (CaR) and Sheba (ShR) ridges at the Aden–Owen–Carlsberg (AOC) triple junction. For each of these three cases, the expected RRF triple junction does not exist because the transform fault arm of the triple junction has evolved into a divergent boundary. AF is Africa plate. AN, Antarctic plate; AR, Arabia plate; EU, Eurasia plate; IN, India plate; JF, Juan Fernandez microplate; NA, North America plate; NZ, Nazca plate; PA, Pacific plate; SO, Somalia plate; TeR, Terceira rift.

in the NW Indian Ocean, which connects the Owen fracture zone (OFZ), the Carlsberg Ridge and the Sheba Ridge (Gordon & DeMets, 1989).

The existence of RRF or ridge–fault–fault (RFF) triple junctions has also long been inferred from the reconstruction of past plate motions from seafloor magnetic anomalies. Based on reconstructions from Chron 5 to 6, Mitchell *et al.* (2000) concluded that the Bouvet triple junction had probably been of the RFF type for 10 m.y. Similarly, Dyment (1993) reconstructed the evolution of the Indian Ocean triple junction in the early Tertiary and identified several successive RFF configurations. An RFF configuration has also been proposed for the Macquarie triple junction (Falconer, 1972) and the 16°40′S triple junction in the North Fiji Basin (Lafoy *et al.*, 1990).

Kinematically, in the hypothesis of symmetrical and orthogonal spreading, a RRF triple junction is generally unstable, except in the rare case of two perpendicular ridges (McKenzie & Morgan, 1969). It is supposed to evolve into a RFF triple junction, which is stable if the velocity–space diagram is isosceles or if the two transform faults have the same strike (flat velocity–space diagram; Patriat & Courtillot, 1984). Actually, in each of the previous three active examples, the expected RFF triple junction does not exist because the transform fault arm of the triple junction has evolved into a divergent boundary. In the case

of the Azores triple junction, the Gloria Transform ends westwards in the oblique Terceira Rift (Vogt & Jung, 2004). At the Juan Fernandez triple junction, a spreading ridge developed at the western end of the Chile Transform, isolating the Juan Fernandez microplate from the Nazca, Pacific and Antarctic plates (Bird *et al.*, 1998). Here, we investigate the case of the AOC triple junction from marine data acquired aboard the *R/V Beautemps-Beaupré* in autumn 2006 (AOC cruise). Before our survey, little was known about this poorly characterized part of the global plate boundary system. We mapped the triple junction with a Kongsberg–Simrad EM120 deep-water multibeam echo-sounder, complemented by gravity, magnetic and sub-bottom seismic profiles. Our data reveal that a large rift basin is developing at the southern end of the OFZ, initiating an ultra-slow divergent boundary between Arabia and India. Consequently, none of the Azores, Juan Fernandez or AOC triple junctions is of RRF type.

GEODYNAMIC SETTING OF THE AOC TRIPLE JUNCTION

In the mouth of the Gulf of Aden, the AOC triple junction connects the OFZ and the Carlsberg and Sheba ridges (Fig. 2). The Carlsberg Ridge, so named by Schmidt
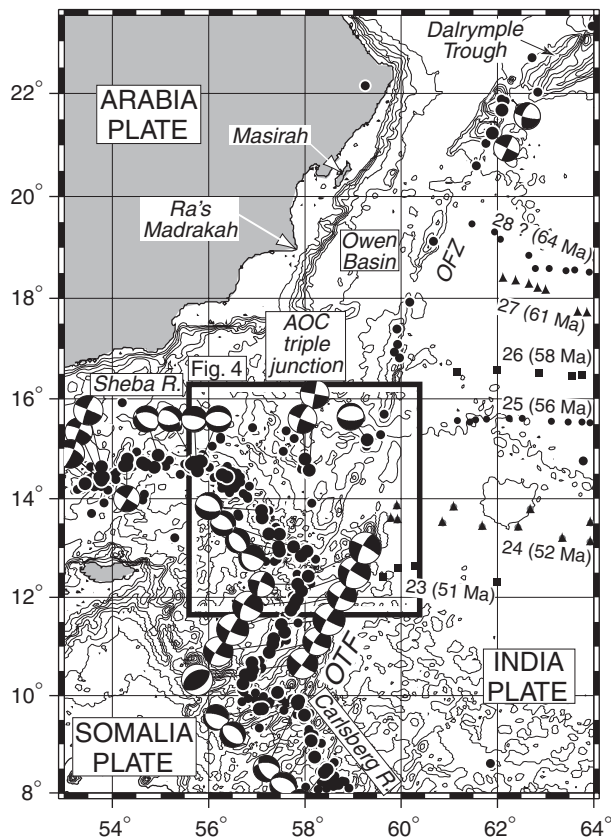
Fig. 2. Geodynamic setting of the Aden–Owen–Carlsberg (AOC) triple junction between the Arabia, India and Somalia plates, with shallow seismicity between 1964 and 1998 (Engdahl *et al.*, 1998; focal depth < 50 km; magnitude > 3.9) and all available earthquake focal mechanisms for the AOC triple junction (Dziewonski *et al.*, 1981; Quittmeyer & Kafka, 1984). The Owen fracture zone (OFZ) is dextral. The Owen transform fault (OTF), which connects the Carlsberg and Sheba ridges, is sinistral. South of 15°N, the southern OFZ is seismically quiet over 250 km. Immediately east of the OFZ, solid symbols correspond to pickings of Early Tertiary magnetic anomalies 23 to possibly 28 identified beneath the Indus Fan (Chaubey *et al.*, 2002; Royer *et al.*, 2002). The location of the ophiolites emplaced along the Oman continental margin in Masirah Island and Ra's Madrakah at the K/T transition is shown. Unlike the Semail ophiolites in northern Oman of Late Cretaceous age, these ophiolites correspond to an ancient oceanic crust of Late Jurassic age (Smewing *et al.*, 1991; Peters & Mercolli, 1998; see Fournier *et al.*, 2006 for a synthesis).

(1932) in honour of the brewer who sponsored his oceano-graphic expeditions, was emplaced in the Early Tertiary between the Seychelles and Indian continental blocks (Norton & Sclater, 1979; Royer *et al.*, 2002). It underwent a three-stage evolution with a fast (half-rate *ca.* 6 cm year^{-1}) spreading stage between 61 and 51 Ma (A27–A23), followed by a very slow (< 0.6 cm year^{-1}) divergence between 39 and 23 Ma (A18–A6b) at the time of collision of India and Eurasia, and by a slow (*ca.* 1.2 cm year^{-1}) spreading stage until

the present (Mercuriev *et al.*, 1996). It is presently characterized by orthogonal accretion at a full rate of 2.2 ± 0.1 cm year^{-1} in its northwestern part (Merkouriev & DeMets, 2006).

The transition from stages 2 to 3 is synchronous with spreading initiation in the eastern Gulf of Aden, where magnetic anomaly 6 (20 Ma) has been identified during the AOC cruise at 58°E. After rifting and break-up of the African continental lithosphere in the Aden rift (Lepvrier *et al.*, 2002; Fournier *et al.*, 2004, 2007; Bellahsen *et al.*, 2006; Gunnell *et al.*, 2007; Petit *et al.*, 2007; Tiberi *et al.*, 2007), the nascent Sheba Ridge, first recognized by Matthews *et al.* (1967) and Laughton *et al.* (1970), rapidly propagated westward (~200 km Ma^{-1}), as indicated by the age of the oldest magnetic anomaly identified in the Gulf of Aden at the longitude of 54°E (An 5D, 17–18 Ma; Leroy *et al.*, 2004; d'Acremont *et al.*, 2006) and 51°E (An 5C, 16 Ma; Sahota, 1990; Huchon & Khanbari, 2003). Accretion at the Sheba Ridge is presently oblique at a poorly constrained full rate of about 2.5 cm year^{-1} in its easternmost end.

The OFZ and the Dalrymple Trough mark the boundary between the Arabian and Indian plates (Fig. 2). This ~700-km-long fault was surveyed in the early sixties by the *H.M.S. Owen* and the *H.M.S. Dalrymple* and subsequently named by Matthews (1966). The OFZ was early recognized by Wilson (1965), in his seminal article on transform faults, as a type example of ridge–trench transform fault that transformed the India–Somalia divergent motion along the Carlsberg Ridge (constructive plate boundary) into the India–Eurasia convergent motion in the Himalayan collision zone (destructive boundary). Physiographically, the India–Arabia boundary consists in a topographic ridge with a curved shape in map view named the Owen Ridge (Whitmarsh *et al.*, 1974). The Owen Ridge is bounded on its eastern side by the OFZ. From correlations of seismic reflection profiles with DSDP Leg 23 borehole data, Whitmarsh *et al.* (1974) dated the uplift of the Owen Ridge as Early Miocene (see also Mountain & Prell, 1990). This age coincides with the rifting to spreading transition in the eastern Gulf of Aden. The OFZ terminates northwards into the Dalrymple Trough (McKenzie & Sclater, 1971), which consists of two sub-basins: a long and narrow basin with a half-graben structure to the south and a rhomboedric-shaped pull-apart basin to the north (Minshull *et al.*, 1992; Edwards *et al.*, 2000; Gaedicke *et al.*, 2002a, b; Ellouz-Zimmermann *et al.*, 2007). Oblique extensional features observed on seismic profiles are compatible with right-lateral motion and a minimum total extension of 5–7 km was estimated across the Dalrymple Trough (Edwards *et al.*, 2000). Southwards, the OFZ joins the Carlsberg and Sheba ridge system at the AOC triple junction (Fournier *et al.*, 2001). The segment of the OFZ running southward from the Dalrymple Trough to the latitude of 15°N is characterized by a low seismic activity (Fig. 2). Further south, the OFZ is seismically quiet for about 250 km. In this area, the Arabia–India plate boundary is not delineated by a well-defined seismic zone.

Earthquake focal mechanisms indicate right-lateral slip along the active segment of the OFZ (Sykes, 1968; Quittmeyer & Kafka, 1984; Gordon & DeMets, 1989), which implies that Arabia is currently moving northward more rapidly than India with respect to Eurasia. Recently, we used three independent datasets (multibeam bathymetry, earthquakes focal mechanisms and space geodesy) to demonstrate that the OFZ is a pure transform fault that closely follows a small circle centred on a nearby pole of rotation (Fournier *et al.*, 2008). The OFZ is an ultra-slow plate boundary with a rate of motion estimated at 2 mm year^{-1} in NUVEL-1 (DeMets *et al.*, 1990, 1994) and re-evaluated at 3–4 mm year^{-1} from GPS data (Reilinger *et al.*, 2006; Fournier *et al.*, 2008).

Several global and regional plate-motion models allow us to build a velocity–space diagram for the AOC triple junction (DeMets *et al.*, 1990; 1994; Jestin *et al.*, 1994; Fournier *et al.*, 2001; Sella *et al.*, 2002; Kreemer *et al.*, 2003; Nocquet *et al.*, 2006; Reilinger *et al.*, 2006; Vigny *et al.*, 2006). Among these models, some predict a null or left-lateral motion along the OFZ and therefore are not acceptable (Jestin *et al.*, 1994; Sella *et al.*, 2002; Kreemer *et al.*, 2003; Vigny *et al.*, 2006). The others can be used to estimate the mean rates and azimuths of motion between Somalia and India and Somalia and Arabia, and associated standard errors (Fig. 3). The corresponding velocity–space diagram is almost flat because the spreading rates and azimuths along the eastern Sheba and western Carlsberg ridges are very close. In the velocity diagram, the location of Arabia and India plates leaves a wide range of possible rates and azimuths for the Ar-In vector (Fig. 3a). Because of these uncertainties, the triple junction could have evolved as either RFF with a completely flat velocity triangle (Fig. 3b) or RRR with an oblique-spreading ridge at the Arabia–India boundary (Fig. 3c). In the following, we discuss the implications of our new data for the evolution of the triple junction over the past 8 m. y.
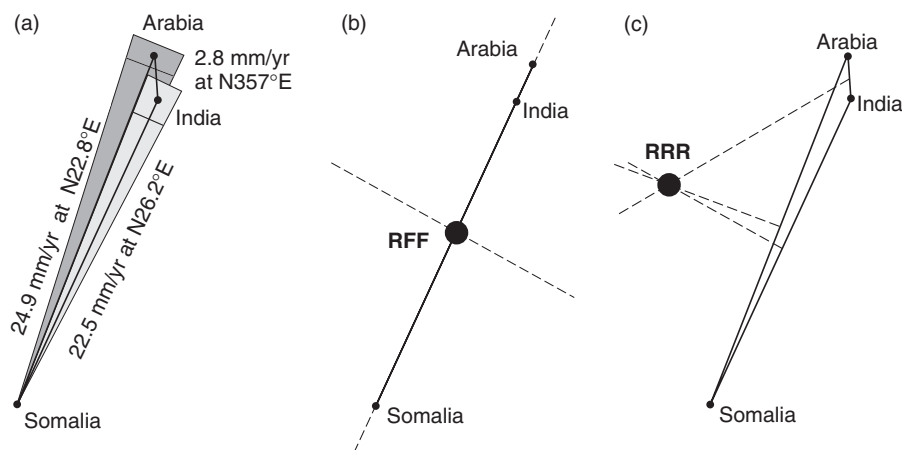
MAIN MORPHOLOGICAL FEATURES OF THE EASTERN SHEBA RIDGE

The axial rift of the eastern Sheba Ridge is underlined by shallow focus earthquakes (Fig. 4). An important seismic swarm observed at 14.4°N and 56.6°E corresponds to a seismic crisis that occurred from 19 to 24 April 1975 (44 earthquakes; $4.5 < m_b < 5.3$), probably related to a dyke intrusion event, based on similarities to seismic swarms associated with dyke intrusions in Iceland (Sykes, 1970; Einarsson, 1986). Focal mechanisms of earthquakes along the axial rift ($4.9 < m_b < 5.8$) are all of normal type (Harvard CMT; Dziewonski *et al.*, 1981), with the exception of two off-axis compressional earthquakes at 13.3°N, which occurred on 22 November 2003. On the multibeam map, the axial rift is sinuous and not segmented by transform faults. The Sheba Ridge deepens towards the SE, where it connects to the Owen transform fault (OTF) through a deep nodal basin (6000 m) named the Wheatley Deep (Matthews *et al.*, 1967).

The eastern Sheba Ridge can be divided into two segments exhibiting distinct morphologic and tectonic features (Fig. 4). West of 57.2°E, the western segment is characterized by a typical morphology of a slow-spreading ridge with a prominent 30–40-km-wide median rift bounded by steeply dipping normal faults stepping down towards the rift axis (Figs 4 and 5a). The axis of spreading is marked by a narrow zone of volcanic activity, which delineates a neovolcanic ridge (Fig. 5a). Along this segment, the axial rift is relatively straight, shallow and continuous, with an N120–130°E trend and depths between 3000 and 3800 m. Linear escarpments corresponding to faults and dykes can be traced for long distances on both sides of the ridge axis. At 14°N and 57°E, the rift axis is offset by a right-stepping, small offset (~10 km) structure, corresponding to a non-transform discontinuity (Macdonald *et al.*, 1988; Spencer *et al.*, 1997; Van Wijk & Blackman, 2005).

Fig. 3. Velocity–space diagrams of the Aden–Owen–Carlsberg (AOC) triple junction. (a) Mean India–Somalia and Arabia–Somalia velocity vectors calculated from DeMets *et al.* (1994), Fournier *et al.* (2001) and Reilinger *et al.* (2006) (solid lines and dots), and associated standard errors (light and dark grey beams, respectively). (b) Possible stable ridge–fault–fault (RFF) configuration with a completely flat velocity triangle. (c) Possible stable ridge–ridge–ridge (RRR) configuration with the mean velocity triangle and an oblique ridge at the Arabia–India boundary.
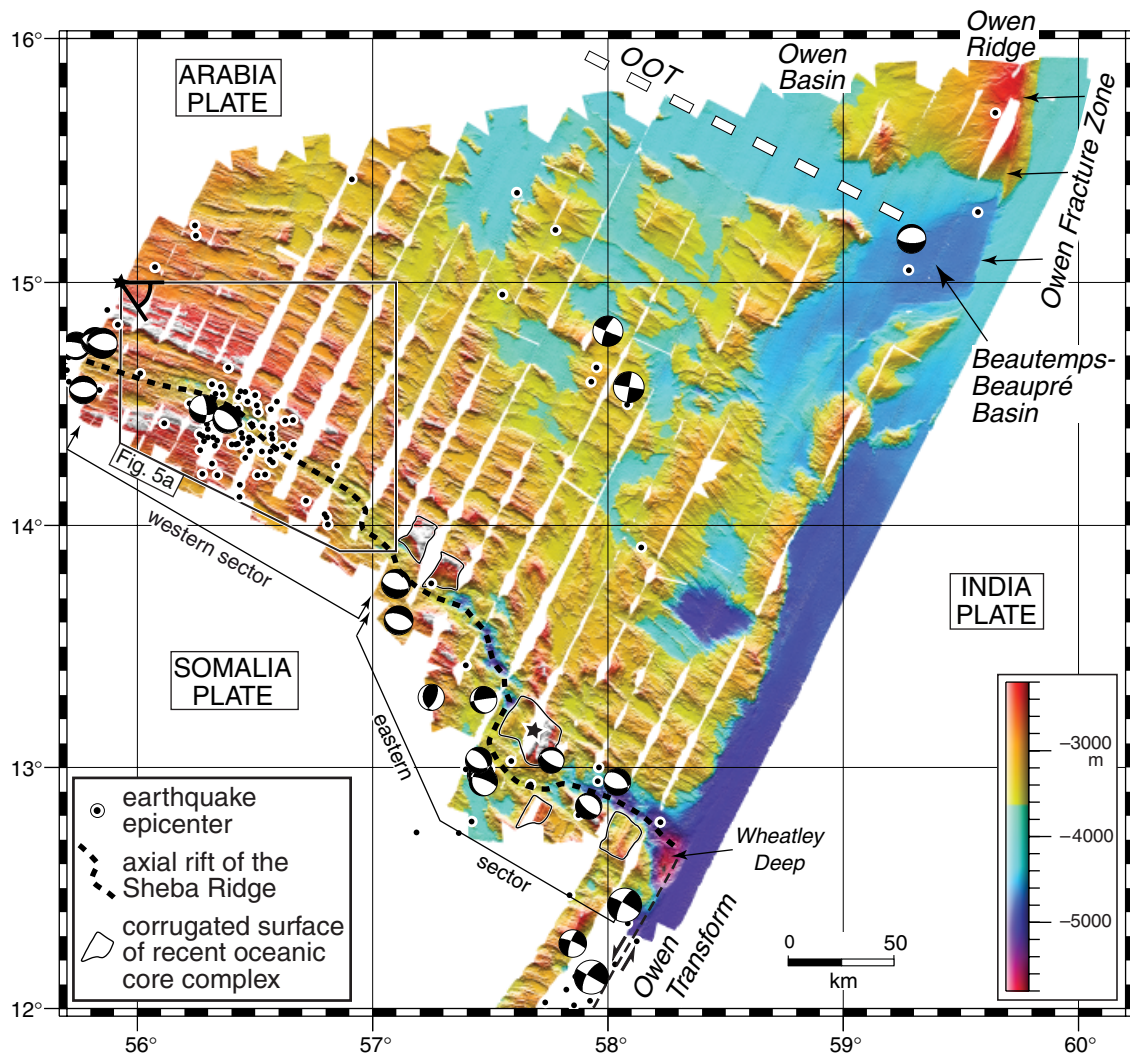
Fig. 4. Multibeam bathymetric map of the Aden–Owen–Carlsberg (AOC) triple junction acquired during the AOC cruise of the *R/V Beautemps-Beaupré* (2006), with shallow seismicity and earthquake focal mechanisms. The map shows the axial rift and the northern flank of the Sheba Ridge, and the southern termination of the Owen fracture zone (OFZ) to the NE. The polygons outline areas of topography that are smooth, rounded (convex upwards) with superimposed ridges and troughs (corrugations) oriented perpendicular to the ridge. These structures are interpreted as oceanic core complexes (or megamullions), as inferred for similar features studied in more detail elsewhere (e.g. Ohara *et al.*, 2001; Searle *et al.*, 2003; Cannat *et al.*, 2006; Ildefonse *et al.*, 2007). OOT is ocean–ocean transition (see text). Star is for location of Fig. 5b.

East of 57.2°E, the axial rift becomes more sinuous and deeper (between 4000 and 4500 m). In this eastern area, the rift basin is bounded alternatively on its northern or southern sides by prominent domes bearing corrugations trending N27°E ± 3°, i.e. parallel to the direction of spreading (Figs 4 and 5b). These structures are interpreted as oceanic core complexes, also named mega-mullions, resulting from the exhumation of lower crustal or upper mantle rocks along low-angle normal faults rooting below the rift valley (Cann *et al.*, 1997; Tucholke *et al.*, 1998). This eastern part is segmented by a large non-transform discontinuity at 13.2°N and 57.5°E where the rift axis is offset by about 25 km (Fig. 4).

The free-air gravity map was built using a Delaunay triangulation method (GMT software, Wessel & Smith, 1991)

with an original data spacing of ∼30 m along the tracks and of ∼17 km between the tracks. The mantle Bouguer anomaly Δmg was computed in the spectral domain using a Fast Fourier Transform algorithm provided by GMT with

$$\Delta mg(k) = 2\pi G[B(k)(\Delta\rho_1 e^{-kd} + \Delta\rho_2 e^{-kl})]$$

where k is the wave number, B is the topography variation (identical for the water/crust and crust/mantle interfaces), G is the gravitational constant, $\Delta\rho_1$ and $\Delta\rho_2$ are the density contrasts for the water/crust and crust/mantle interfaces (1840 and 300 kg m^{-3}, respectively) and d and l are the mean depths of these interfaces (2500 and 7500 m, respectively). The free-air gravity map displays relative highs following the Sheba Ridge topography (Fig. 6). Two elevated peaks of
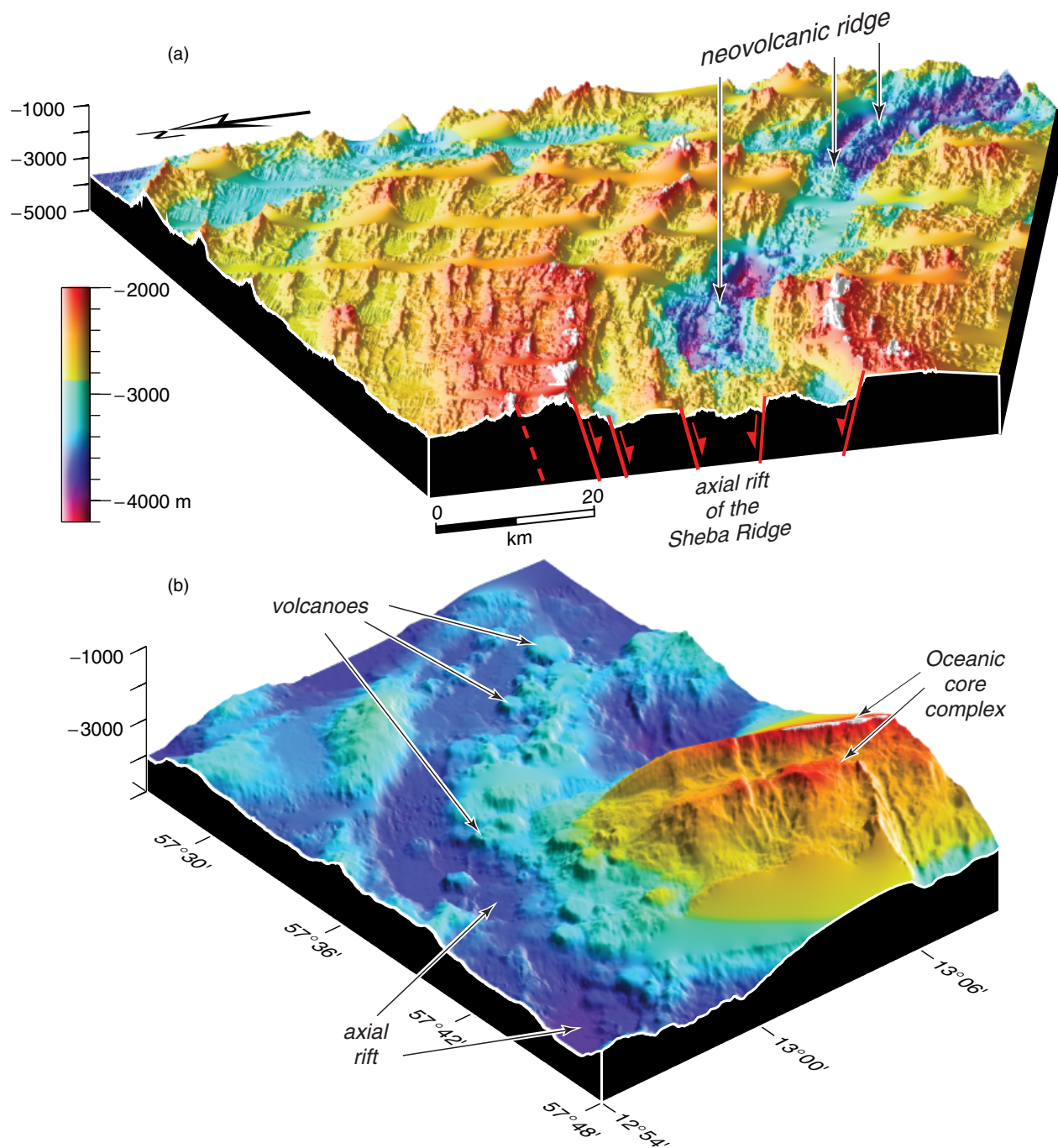
Fig. 5. (a) Perspective view from the NW of the western median rift developed at the Sheba Ridge axis. The rift is 30–40 km wide and 3000–3800 m deep. Away from the neovolcanic ridge, which marks the axis of spreading, the topography is controlled by riftward-dipping normal faults. (b) Volcanoes and oceanic core complexes in the eastern part of the axial rift. Location in Fig. 4. Colour scales in Figs 4 and 5 are different.

more than 60 mGal immediately north of the axial rift correspond to two large oceanic core complexes. A triangular area of negative mantle Bouguer anomaly covers the western part of the Sheba Ridge. On the other hand, positive values are encountered in the eastern part of the surveyed area, except at its northeastern extremity. To first order, mantle Bouguer anomaly variations may reflect crustal thickness variations: the relatively low anomaly found in the western part of the Sheba ridge, correlated with the high topography, could indicate a thick oceanic crust there, whereas the positive anomaly observed on the eastern part of the ridge could be associated with a reduced crustal thickness in the domain where core complex exhumation prevails.
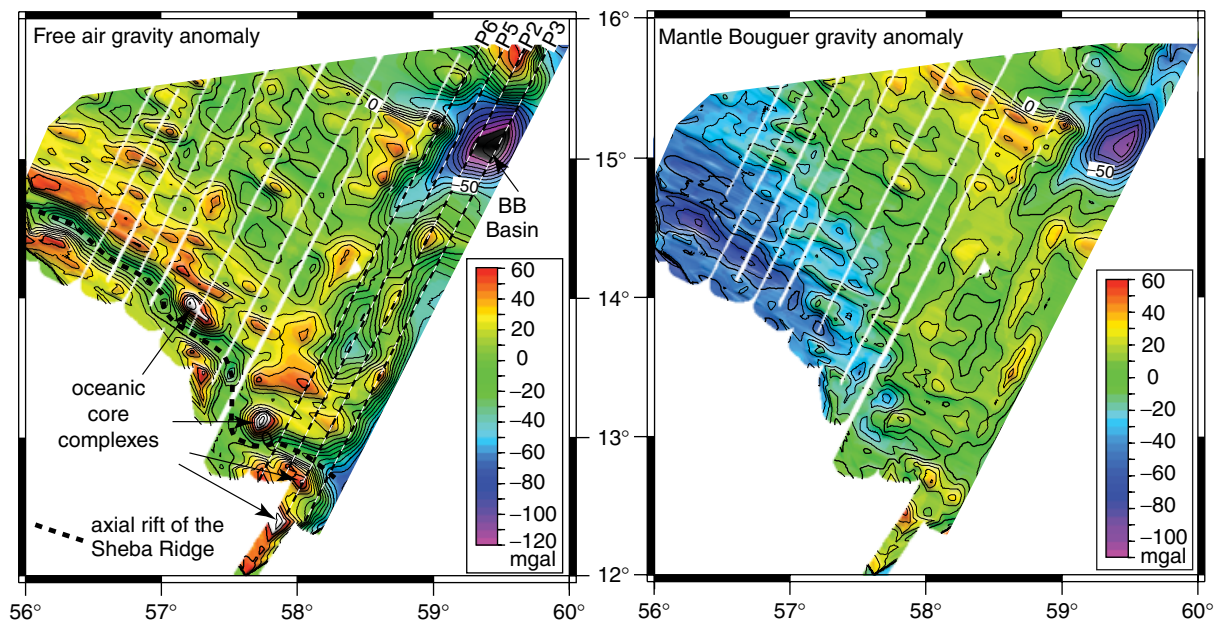
Fig. 6. Free air and mantle Bouguer gravity maps of the Aden–Owen–Carlsberg (AOC) triple junction. Gravity data were acquired along the ship tracks with an original data spacing of 30 m along track and 17 km between tracks and an accuracy of 0.02 mGal. The complete Bouguer gravity was computed by using a mean density contrast of 1840 kg m^{-3} between the oceanic crust and water, and of 300 kg m^{-3} between the crust and mantle. Dashed lines show location of profiles in Fig. 10.

FORMATION OF A RIFT BASIN AT THE SOUTHERN END OF THE OFZ

In the northeastern part of the surveyed area, the southern extremity of the OFZ has been mapped over about 120 km (Figs 4 and 7). The OFZ appears as a rectilinear fault trending N10°E $\pm$ 3° (Fig. 7a). This vertical fault crosscuts the Owen topographic ridge and offsets it dextrally. The total displacement along the fault is estimated from a right-lateral apparent geomorphologic offset of 12 $\pm$ 1 km measured on the multibeam map (Fig. 7b). The fault does not display any noticeable vertical offset. It is a nearly pure strike–slip fault.

To the south, the OFZ forms the eastern margin of a 50-km-wide basin bounded by N70–N90°E-trending normal faults, and connects to the south with the southern border normal faults (Figs 7b and 8). The basin thus consists of a transtensional pull-apart basin that is forming at the southern extremity of the OFZ. We would like to suggest the name of Beautemps–Beaupré Basin for this still un-named feature. Seismicity in the basin and one extensional focal mechanism at the northern edge of the basin (Harvard CMT, 12 September 1990, m_b = 5.5) attest to active normal faulting. The southward steeply dipping nodal plane of the focal mechanism likely corresponds to the bounding fault plane.

Sub-bottom 3.5 kHz profiles reveal the shallow structure of the Beautemps–Beaupré Basin (Fig. 9). In its eastern part, the basin is bounded to the north and the south by two major conjugate normal faults displaying a vertical geomorphologic offset of about 100 m (profile AOC3). This

offset progressively decreases westward and disappears in the western part of the basin (Figs 7b and 9). Inside the basin, numerous minor normal faults with offsets smaller than 10 m crosscut the youngest sedimentary deposits (Fig. 9). Some of them display a downward-increasing offset, which attests to their synsedimentary activity (see the blow-up of profile AOC3 in Fig. 9). On the 3.5 kHz profiles, the basin infill is characterized from top to bottom by a layered seismic sequence with strong reflections overlying two thick transparent layers (tr1 and tr2 in profiles AOC5 and AOC6). The layered sequence may represent turbidites, as multibeam data show that the Beautemps–Beaupré Basin is supplied in turbidity-current deposits by a channel coming from the Indus Fan. The upper transparent layer (tr2) can be correlated from west to east from profiles AOC6 to AOC3, whereas the lower one (tr1) is observed only on profiles AOC5 and AOC6. This observation indicates that sedimentary sequences become thicker from west to east, reflecting an eastward increase of the subsidence rate. The eastern part of the basin is asymmetrical with a larger cumulative normal fault offset in its southern half, at the location of the present-day depocentre (profile AOC3). On the other hand, in its western part, the basin is divided into two sub-basins separated by a central horst, and numerous normal faults are observed on the southern edge of the basin (profile AOC5).

The eastern part of the Beautemps-Beaupré basin is characterized by a strong negative free-air gravity anomaly of $\sim$100 mGal with respect to the surrounding crust, probably due to a thick low-density sedimentary infill
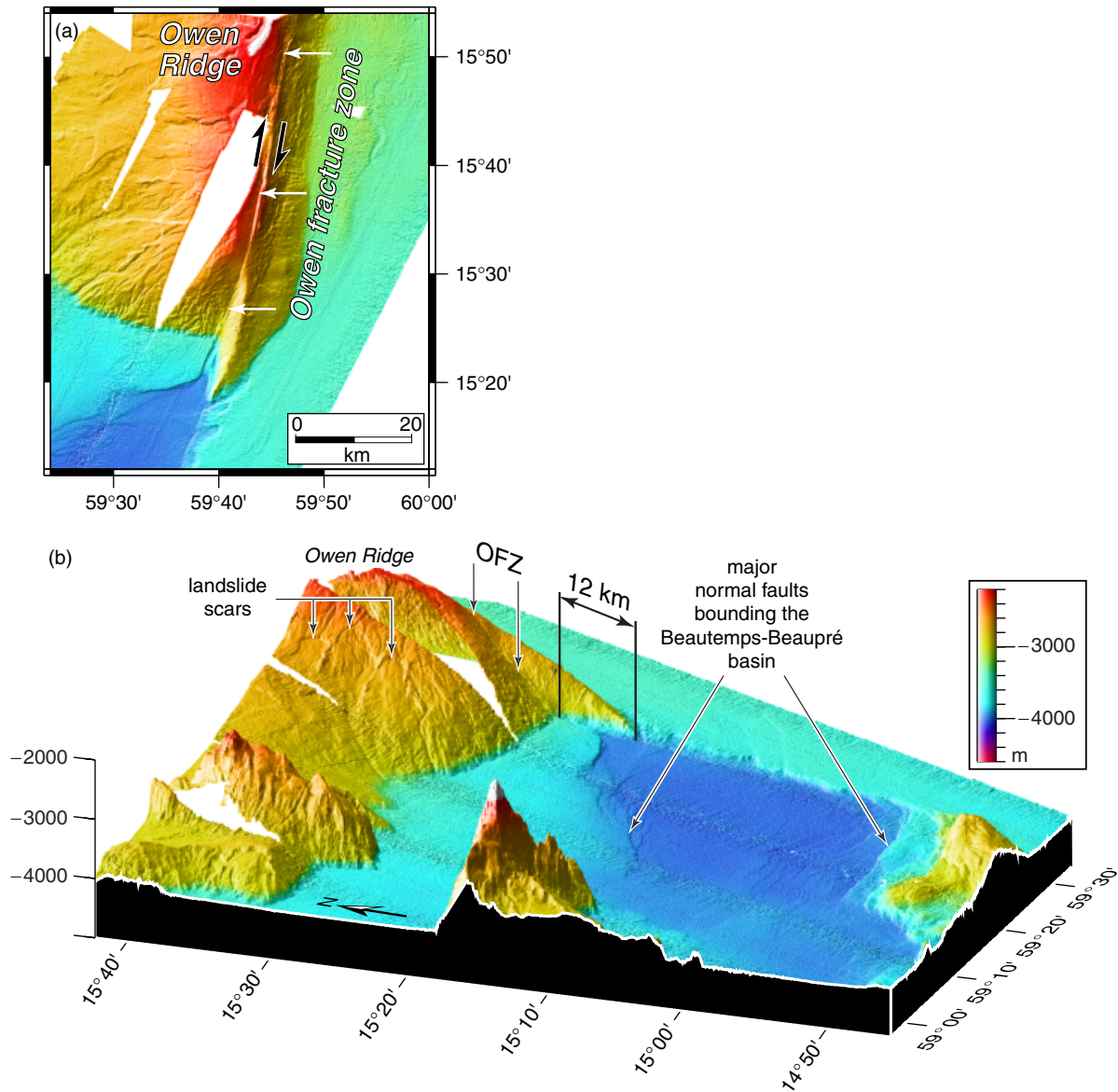
Fig. 7. Perspective views of (a) the N10°E-trending Owen fracture zone (OFZ) offsetting the Owen Ridge over 12 km and (b) the Beautemps–Beaupré rift basin at the southern end of the OFZ bounded by N70–N90°E-trending normal faults.

(Fig. 6 and profiles 2 and 3 in Fig. 10). Moreover, the gravity minimum is offset southwards by about 5 km with respect to the basin centre, suggesting an asymmetrical infill with a greater basement depth to the south, in agreement with the high density of normal faults there. The gravity low in the western part of the basin is about half that of the eastern basin (profiles 5 and 6 in Fig. 10), suggesting a less well-developed basin there in agreement with the westward decreasing subsidence observed on 3.5 kHz profiles. This part of the basin has probably developed recently within the oceanic crust of the northern flank of the Sheba Ridge. In contrast to the sharp eastern border of the basin that forms the active OFZ, its western edge is poorly defined and is marked by numerous landslides on the surrounding oceanic highs (Fig. 8 and profile AOC6). SW of the basin, the oceanic crust is cut by E–W-trending faults offsetting

former structures (dykes and faults) formed at the Sheba Ridge. The extensional deformation thus seems to propagate westward into the oceanic crust, its style evolving from localized to diffuse from east to west. Two large earthquakes with strike–slip focal mechanisms occurred in the area (Figs 4 and 8; Harvard CMT, 5 December 1981, m_b = 5.6; 14 December 1985, m_b = 5.5), but the corresponding fault planes could not be clearly identified on the multibeam map.

In summary, this new set of marine data shows that the southern part of the active OFZ corresponds to a pure right-lateral active fault with a visible finite offset of 12 km. Motion along this fault postdates the uplift of the Owen Ridge. The onset of motion along the fault, obtained by dividing its finite offset by the mean rate of motion, has been estimated between 4 and 8 Ma (Fournier *et al.*,
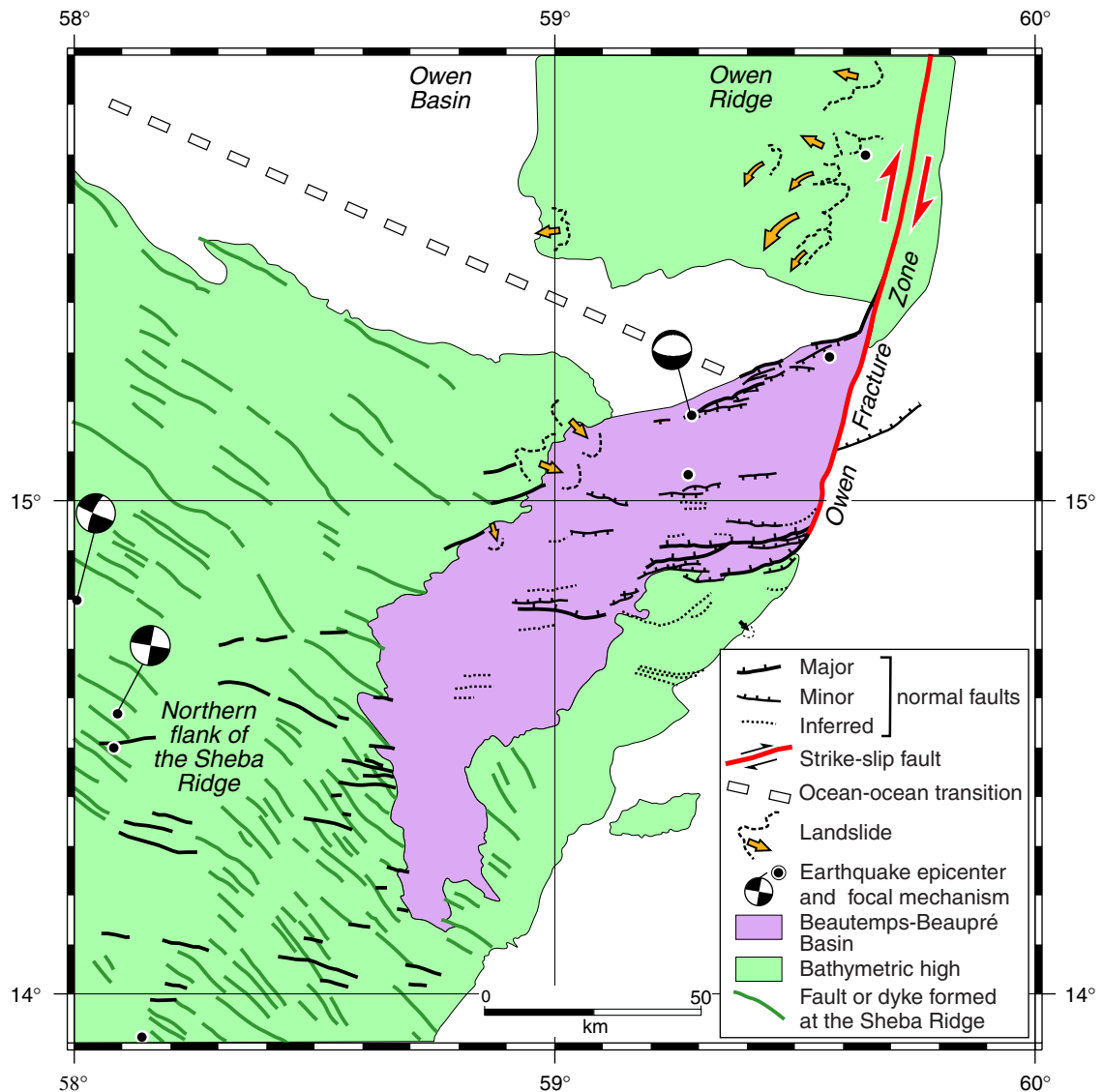
Fig. 8. Structural map of the southern end of the Owen fracture zone (OFZ). The OFZ terminates in the 50-km-wide and 120-km-long Beautemps–Beaupré Basin bounded by normal faults. Rifting was initiated in the transition zone between the young oceanic crust generated at the Sheba Ridge and the old oceanic crust of the Owen Basin. By analogy with the ocean–continent transition (OCT) located westward in the Gulf of Aden, this transition is more properly named 'ocean–ocean transition' (OOT) than pseudofault. Strictly speaking, a pseudofault is defined as the fossil trace ('propagator wake') made by the propagation of a segment of spreading ridge at the expenses of the retreating adjacent segment (Hey, 1977; Kleinrock & Hey, 1989; Kruse *et al.*, 2000; Briais *et al.*, 2002). Here, the OOT corresponds to the transition between a rifted, old oceanic crust formed at a now disappeared spreading ridge and a young oceanic crust newly formed at the Sheba Ridge. The Beautemps–Beaupré rift propagated westward in the oceanic crust of the northern flank of the Sheba Ridge. To the west of the basin, E–W faults in the oceanic crust crosscutting faults and dykes generated at the Sheba Ridge suggest that the extensional deformation is propagating westward. Minor normal faults are also observed to the east of the OFZ on the Indian plate. Numerous landslides probably triggered by earthquakes are observed along the slopes.

2008). The fault terminates into an active rift basin some 250 km north of the Sheba Ridge. The basin probably started to develop 4–8 Ma, together with the active fault. The extensional deformation appears to propagate westward into the oceanic crust, but does not presently join the axial rift of the Sheba Ridge. The AOC triple junction presently corresponds to a widespread zone of distributed deformation.

SUBMARINE LANDSLIDES ALONG THE ACTIVE OFZ

The Owen Ridge is a prominent topographic ridge of 2000 m height with respect to the surrounding seafloor. Seismic profiles indicate that the ridge is asymmetric with a steep east-facing scarp associated with the OFZ and a gentle western slope corresponding to sedimentary beds
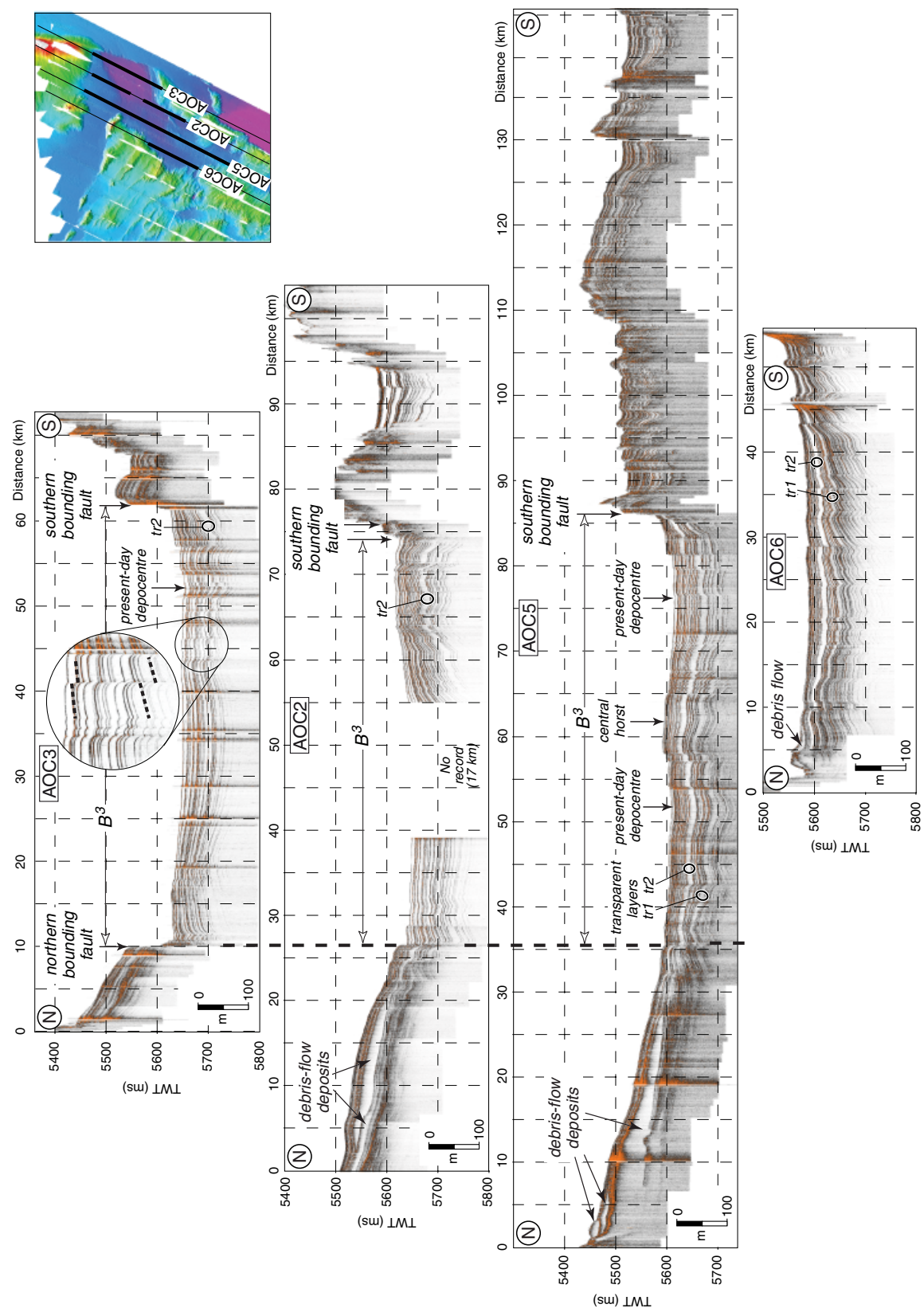
Fig. 9. High–resolution (3.5 kHz) seismic reflection profiles across the Beautemps–Beaupré Basin. The profiles are aligned on the northern bounding fault of the basin. The blow-up on profile AOC3 illustrates the downward increasing offset of a synsedimentary normal fault. B³ is Beautemps–Beaupré Basin. Location of profiles is shown in inset.
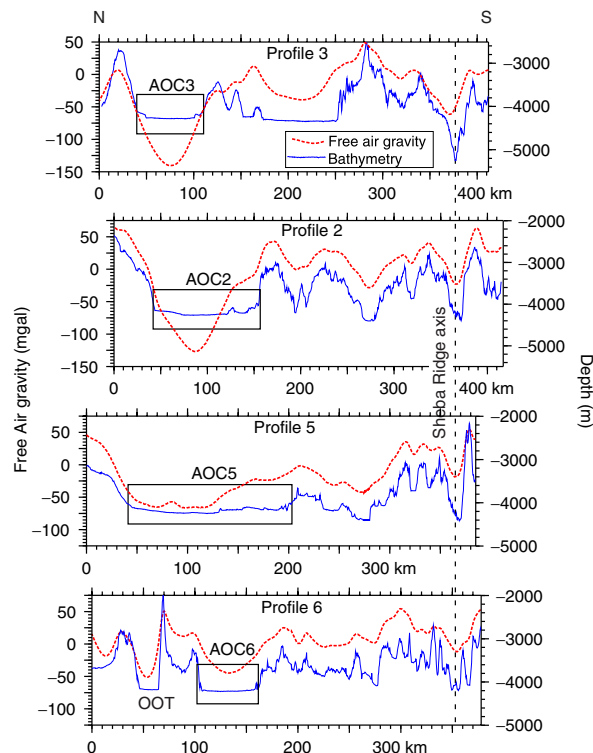
Fig. 10. Free air gravity and bathymetry profiles across the Beautemps–Beaupré Basin and the northern flank of the Sheba Ridge. Profiles are oriented along N27°E and aligned on the ridge axis. Location of profiles is shown in Fig. 6.
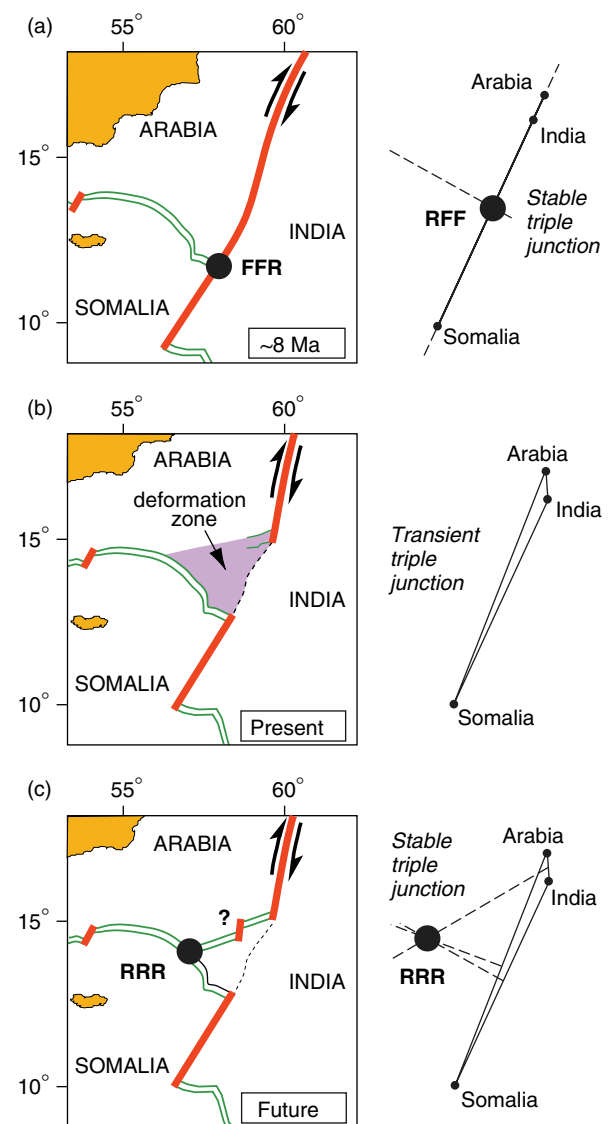

Fig. 11. Sketch of successive stages of evolution of the triple junction since ∼8 Ma with corresponding velocity triangle and stability of the triple junction. The configuration of the junction before (a) and after (b) the development of the pull-apart basin is shown, and a possible ridge–ridge–ridge (RRR) configuration (c) in the near future is proposed. The change in configuration of the triple junction was probably induced by a regional reorganization of plate velocities and directions 8–10 Ma, which initiated the active strike–slip fault and the pull-apart basin. The dashed lines represent velocities, which leave the geometry of the boundaries unchanged.

tilted a few degrees towards the west (Whitmarsh *et al.*, 1974; Mountain & Prell, 1990). On the western slope, seismic profiles acquired during the DSDP Leg 23 showed that the uppermost sediments have been stripped off without disturbing underlying reflectors, presumably by sliding of non-competent beds over more competent beds. The scarps produced at the point of detachment of the upper layers have been observed on seismic profiles (Whitmarsh *et al.*, 1974). Our multibeam data also reveal several sinuous headwall scars of landslide on the western slope of the Owen Ridge (Fig. 7b). After failure on the slope, these landslides must have generated typical slope deposits such as debrites (the deposit formed by a debris flow) and turbidites. On the northern margin of the Beautemps–Beaupré Basin, the thick lens-shaped sediment bodies displaying a transparent seismic facies on 3.5 kHz profiles (profiles AOC2 and AOC5 in Fig. 9) may correspond to debrites, by analogy with similar deposits unequivocally identified as debrites by coring (Lastras *et al.*, 2004; Talling *et al.*, 2007). On the AOC5 profile, three superimposed transparent bodies separated by thin-layered sequences attest to frequent landslides on the Owen Ridge. The largest debris-flow deposit, which is also laterally observed on profile AOC2, is about 30 m thick (assuming a mean sound speed of $1800 \, \mathrm{m \, s^{-1}}$). The fine-grained portion of the debris flow might have been deposited further south in the deep basin and could correspond to the thick transparent layers (tr1 and tr2) observed on the

3.5 kHz profiles. Giant landslides along the Owen Ridge are probably triggered by earthquakes occurring along the OFZ or along the normal faults of the basin.

DISCUSSION: DEVELOPMENT OF AN ULTRA-SLOW DIVERGENT PLATE BOUNDARY

Rift nucleation at the ocean–ocean transition (OOT)

At the southern end of the OFZ, rifting localizes at the transition zone between the recent oceanic crust created

at the Sheba Ridge and a crust of different origin pertaining to the Owen basin (Fig. 2). The latter, located between the OFZ and the Arabian continental margin (Oman margin), is mainly floored with oceanic crust as indicated by seismic reflection and refraction data (Whitmarsh, 1979; Stein & Cochran, 1985; Barton *et al.*, 1990). Its age remains poorly constrained, however, because it lacks clearly identified sequences of lineated magnetic anomalies. It could correspond to the ancient passive margin of the Africa–Arabia continent formed during the break-up of Gondwanaland (Whitmarsh, 1979; Stein & Cochran, 1985). In this case, the crust would be of Late Jurassic–Early Cretaceous age like the North Somali Basin (Bunce *et al.*, 1967; Cochran, 1988) and like the ophiolites emplaced on the Oman margin in Masirah Island and Ra's Madrakah (Fig. 2; Beurrier, 1987; Smewing *et al.*, 1991; Peters & Mercolli, 1998). However, the unloaded basement depth in the Owen basin is more than 1 km shallower than expected for an oceanic crust of Jurassic age (Mountain & Prell, 1990). Moreover, the correlation of seismic profiles with the DSDP 224 drilling rather supports a Late Cretaceous or a younger age for the basement of the Owen basin (see Edwards *et al.*, 2000 for a synthesis). Whatever its age, this ancient oceanic lithosphere was rifted apart in the Early Miocene to form the easternmost segment of the Sheba Ridge between the eastern edges of Arabia and Africa to the OFZ. The newly formed Beautemps–Beaupré rift basin nucleated at the transition zone between the old oceanic lithosphere of the Owen Basin and the Miocene oceanic lithosphere of the Sheba Ridge, i.e. in the OOT zone, by analogy with the ocean–continent transition (OCT) at the foot of the rifted continental margin of the Gulf of Aden (d'Acremont *et al.*, 2005; see also Shillington *et al.*, 2006). In the eastern Gulf of Aden, the OOT nearly coincides with the 'magnetic quiet zone' described by Cochran (1981, 1982). The OOT appears as a zone of rheological weakness where intra-oceanic rifting was initiated some 4–8 Ma, before propagating westward in the oceanic lithosphere of the northern Sheba Ridge.

Is the present-day AOC triple junction stable or transient?

On the multibeam map (Fig. 4), there is no evidence of active deformation along the seismically quiet segment of the OFZ between 12.8°N and 15°N, which separates the oceanic lithosphere formed at the Sheba Ridge to the west from that formed at the Carlsberg Ridge to the east. The Arabia–India plate boundary terminates into the Beautemps–Beaupré rift basin some 250 km north of the Sheba Ridge and it is diffuse and not marked by a well-defined seismic zone between the BB Basin and the ridge axis (Fig. 11b).

Before the initiation of the new plate boundary fault (i.e. 4–8 Ma), the southern segment of the OFZ between 12.8°N and 15°N was probably active and accommodated the Arabia–India dextral relative motion inferred from magnetic data from the Sheba and Carlsberg ridges (Gor-

don & DeMets, 1989). The AOC triple junction was then located at the junction of the old OFZ, the Sheba Ridge and the OTF with a RFF geometry (Fig. 11a). Because this kind of triple junction is often unstable, it was probably abandoned when a change of the Arabia–India kinematics caused the activation of the newly imaged fault, together with the formation of the Beautemps–Beaupré Basin. The latest kinematic reorganization in the Indian Ocean occurred ∼8 Ma and corresponds to the onset of intraplate deformation in the India–Australia plate dated at 7.5–8 Ma by ODP drillings (Cochran, 1990; Chamot-Rooke *et al.*, 1993; Delescluse & Chamot-Rooke, 2007), which nearly coincides with kinematic change along the Carlsberg Ridge between 11 and 9 Ma (Merkouriev & DeMets, 2006).

The Beautemps–Beaupré rift basin was initiated at the OOT and propagated westward into the Arabian plate interior. An ultraslow divergent boundary is therefore developing between Arabia and India and might join the Sheba Ridge axis in the future to reach a more stable RRR triple junction (Fig. 11c). Part of the Arabian plate is thus being transferred to the Indian plate (DeMets, 2008). At present, deformation is not clearly localized between the BB Basin and the Sheba Ridge, and the current configuration of the triple junction appears as a transient state preceding the establishment of a new divergent plate boundary.

Future evolution of the AOC triple junction

As shown in Fig. 1, the geometry of the AOC triple junction is the same as that of the Azores triple junction rotated counterclockwise by 90°. Moreover, the Africa–Iberia–North America triple junction that existed when Iberia was moving independently from Eurasia at the time of opening of King's Trough, from 44 to 25 Ma, also had a similar geometry with an oblique rift – King's Trough – connecting a transform fault to the MAR (Srivastava *et al.*, 1990). This geometry thus seems to be common in the context of connection of a transform fault with a spreading ridge. Another similarity between the AOC and Azores triple junctions is their plate velocity–space diagrams, with two slow-spreading ridges having similar rates and directions and one ultraslow spreading boundary forming the third arm (Searle, 1980). The main difference between the two triple junctions is the existence of a hot spot beneath the Azores triple junction. The Azores triple junction, with its well-developed Terceira rift, might represent a future stage of development of the AOC triple junction. Then, the rift arm of the Azores and AOC triple junctions could evolve into an oceanic spreading centre, like for the Juan Fernandez triple junction, where a spreading ridge developed at the termination of the Chile Transform.

CONCLUSION

Do RRF (or RFF) triple junctions really exist on Earth? Among the three known active examples of such triple junctions, previous studies have demonstrated that two of

them are actually of the RRR type. Our study shows that the last one – the AOC triple junction in the Indian Ocean – is also evolving into an RRR-type junction. As a consequence, despite the fact that the regional plate configuration and far-field kinematics may define an RRF or RFF connection, the local geometry of the triple junction is always of RRR type. The substitution of RRF (or RFF) triple junctions by more stable RRR triple junctions with a rift arm may be a mechanical adaptation of the oceanic lithosphere to changing kinematic boundary conditions.

ACKNOWLEDGEMENTS

REFERENCES

ARGUS, D.F., GORDON, R.G., DEMETS, C. & STEIN, S. (1989) Closure of the Africa–North America plate motion circuit and tectonics of the Gloria fault. *J. Geophys. Res.*, **94**, 5585–5602.

BARTON, P.J., OWEN, T.R.E. & WHITE, R.S. (1990) The deep structure of the east Oman continental margin: preliminary results and interpretation. *Tectonophysics*, **173**, 319–331.

BELLAHSEN, N., FOURNIER, M., D'ACREMONT, E., LEROY, S. & DANIEL, J.-M. (2006) Fault reactivation and rift localization: The northeastern Gulf of Aden margin. *Tectonics*, **25**, doi:10.1029/2004TC001626.

BEURRIER, M. (1987) Géologie de la nappe ophiolitique de Semail dans les parties orientales et centrales de l'Oman, Thèse Doc. Etat, University of Paris 6, 406pp.

BIRD, R.T. & NAAR, D.F. (1994) Intratransform origins of mid-ocean ridge microplates. *Geology*, **22**, 987–990.

BIRD, R.T., NAAR, D.F., LARSON, R.L., SEARLE, R.C. & SCOTESE, C.R. (1998) Plate tectonic reconstructions of the Juan Fernandez microplate: transformation from internal shear to rigid rotation. *J. Geophys. Res.*, **103**, 7049–7067.

BRIAIS, A., ASLANIAN, D., GÉLI, L. & ONDRÉAS, H. (2002) Analysis of propagators along the Pacific–Antarctic Ridge: evidence for triggering by kinematic changes. *Earth Planet. Sci. Lett.*, **199**, 415–428.

BUNCE, E.T., LANGSETH, M.G., CHASE, R.L. & EWING, M. (1967) Structure of the Western Somali Basin. *J. Geophys. Res.*, **72**, 2547–2555.

CANN, J.R., BLACKMAN, D.K., SMITH, D.K., MCALLISTER, E., JANSSEN, B., MELLO, S., AVGERINOS, E., PASCOE, A.R. & ESCARTIN, J. (1997) Corrugated slip surfaces formed at ridge-transform intersections on the Mid-Atlantic Ridge. *Nature*, **385**, 329–332.

CANNAT, M., SAUTER, D., MENDEL, V., RUELLAN, E., OKINO, K., ESCARTIN, J., COMBIER, V. & BAALA, M. (2006) Modes of sea floor generation at a melt-poor ultraslow-spreading ridge. *Geology*, **34**, 605–608.

CHAUBEY, A.K., DYMENT, J., BHATTACHARYA, G.C., ROYER, J.-Y., SRINIVAS, K. & YATHEESH, V. (2002) Paleogene magnetic isochrons and paleo-propagators in the Arabian and Eastern Somali basins, Northwest Indian Ocean. In: *The Tectonic & Climatic Evolution of the Arabian Sea Region* (Ed. by P. Clift, D. Kroon, C. Gaedicke & J. Craig), *Geol. Soc. Spec. Publ.*, **195**, 71–85.

CHAMOT-ROOKE, N., JESTIN, F. & DE VOOGD, B. THE PHÈDRE WORKING GROUP. (1993) Intraplate shortening in the central Indian Ocean determined from 2100-km-long north–south deep seismic rection prole. *Geology*, **21**, 1043–1046.

COCHRAN, J.R. (1981) The Gulf of Aden: structure and evolution of a young ocean basin and continental margin. *J. Geophys. Res.*, **86**, 263–287.

COCHRAN, J.R. (1982) The magnetic quiet zone in the eastern of the Gulf of Aden: implications for the early development of the continental margin. *Geophys. J. Royal Astronom. Soc.*, **68**, 171–201.

COCHRAN, J.R. (1988) Somali Basin, Chain Ridge, and origin of the Northern Somali Basin gravity and geoid low. *J. Geophys. Res.*, **93**, 11985–12008.

COCHRAN, J.R. (1990) Himalayan uplift, sea level, and the record of Bengal Fan sedimentation at the ODP LEG 116 Sites. *Proc. Ocean Drilling Progr. Sci. Res.*, **116**, 397–414.

D'ACREMONT, E., LEROY, S., BESLIER, M.-O., BELLAHSEN, N., FOURNIER, M., ROBIN, C., MAIA, M. & GENTE, P. (2005) Structure and evolution of the eastern Gulf of Aden conjugate margins from seismic reflection data. *Geophys. J. Int.*, **160**, 869–890.

D'ACREMONT, E., LEROY, S., MAIA, M., PATRIAT, P., BESLIER, M.-O., BELLAHSEN, N., FOURNIER, M. & GENTE, P. (2006) Structure and evolution of the eastern Gulf of Aden: insights from magnetic and gravity data (Encens Sheba Cruise). *Geophys. J. Int.*, **165**, 786–803.

DELESCLUSE, M. & CHAMOT-ROOKE, N. (2007) Instantaneous deformation and kinematics of the India–Australia Plate. *Geophys. J. Int.*, **168**, 818–842.

DEMETS, C. (2008) Arabia's slow danse with India. *Nat. Geosci.*, **1**, 10–11, doi:10.1038/ngeo.2007.56.

DEMETS, C., GORDON, R.G., ARGUS, D.F. & STEIN, S. (1990) Current plate motions. *Geophys. J. Int.*, **101**, 425–478.

DEMETS, C., GORDON, R.G., ARGUS, D.F. & STEIN, S. (1994) Effect of recent revisions of the geomagnetic reversal time scale on estimates of current plate motions. *Geophys. Res. Lett.*, **21**, 2191–2194.

DYMENT, J. (1993) Evolution of the Indian Ocean Triple junction between 65 and 49 Ma (anomalies 28 to 21). *J. Geophys. Res.*, **98**, 13863–13877.

DZIEWONSKI, A.M., CHOU, T.A. & WOODHOUSE, J.H. (1981) Determination of earthquake source parameters from waveform data for studies of global and regional seismicity. *J. Geophys. Res.*, **86**, 2825–2852.

EDWARDS, R.A., MINSHULL, T. & WHITE, R.S. (2000) Extension across the Indian–Arabian plate boundary: the Murray Ridge. *Geophys. J. Int.*, **142**, 461–477.

EINARSSON, P. (1986) Seismicity along the eastern margin of the North American plate. In: *The Geology of North America: Vol. M, The Western North Atlantic Region* (Ed. by P.R. Vogt & B.E. Tucholke), pp. 99–116. The Geological Society of America, Boulder, CO.

ELLOUZ-ZIMMERMANN, N., LALLEMANT, S., CASTILLA, R., MOUCHOT, N., LETURMY, P., BATTANI, A., BURET, C., CHEREL, L., DESAUBLIAUX, G., DEVILLE, E., FERRAND, J., LUQCKE, A., MAHIEUX, G., MASCLE, G., MUHR, P., PIERSON-WICKMANN, A., ROBION, P., SCHMITZ, J., DANISH, M., HASANV, S., SHAHZAD, A. & TABREEZ, A. (2007) Offshore frontal part of the Makran Accretionary prism: the Chamak survey (Pakistan). In: *Thrust Belts and Foreland Basins – From Fold Kinematics to Hydrocarbon System, Frontiers in Earth Science Series* (Ed. by O. Lacombe, J. Lavé, F. Roure & J. Vergés), pp. 351–366. Springer, Heidelberg.

ENGDAHL, E.R., VAN DER HILST, R. & BULAND, R. (1998) Global teleseismic earthquake relocation with improved travel times and procedures for depth determination. *Bull. Seismol. Soc. Am.*, **88**, 722–743.

FALCONER, R.K.H. (1972) The Indian–Antarctic–Pacific Triple Junction. *Earth Planet. Sci. Lett.*, **17**, 151–158.

FERNANDES, R.M.S., BASTOS, L., MIRANDA, J.M., LOURENÇO, N., AMBROSIUS, B.A.C., NOOMEN, R. & SIMONS, W. (2006) Defining the plate boundaries in the Azores region. *J. Volc. Geotherm. Res.*, **156**, 1–9.

FOURNIER, M., BELLAHSEN, N., FABBRI, O. & GUNNELL, Y. (2004) Oblique rifting and segmentation of the NE Gulf of Aden passive margin. *Geochem. Geophys. Geosyst.*, **5**, Q11005, doi:10.1029/2004GC000731.

FOURNIER, M., CHAMOT-ROOKE, N., PETIT, C., FABBRI, O., HUCHON, P., MAILLOT, B. & LEPVRIER, C. (2008) In-situ evidence for dextral active motion at the Arabia–India plate boundary. *Nat. Geosci.*, **1**, 54–58, doi:10.1038/ngeo.2007.24.

FOURNIER, M., HUCHON, P., KHANBARI, K. & LEROY, S. (2007) Segmentation and along-strike asymmetry of the passive margin in Socotra, eastern Gulf of Aden: are they controlled by detachment faults? *Geochem. Geophysics Geosystems*, **8**, Q03007, doi:10.1029/2006gc001526.

FOURNIER, M., LEPVRIER, C., RAZIN, P. & JOLIVET, L. (2006) Late Cretaceous to Paleogene post-obduction extension and subsequent Neogene compression in the Oman Mountains. *GeoArabia*, **11**, 17–40.

FOURNIER, M., PATRIAT, P. & LEROY, S. (2001) Reappraisal of the Arabia–India–Somalia Triple Junction kinematics. *Earth Planet. Sci. Lett.*, **189**, 103–114.

GAEDICKE, G., PREXL, A., SCHLÜTER, H.-U., MEYER, H., ROESER, H.A. & CLIFT, P. (2002a) Seismic stratigraphy and correlation of major regional unconformities in the northern Arabian Sea. *Geol. Soc. London Spec. Pub.*, **195**, 25–36.

GAEDICKE, G., SCHLÜTER, H.-U., ROESER, H.A., PREXL, A., SCHRECKENBERGER, B., MEYER, H., REICHERT, C., CLIFT, P. & AMJAD, S. (2002b) Origin of the northern Indus Fan and Murray Ridge, Northern Arabian Sea: interpretation from seismic and magnetic imaging. *Tectonophysics*, **355**, 127–143.

GORDON, R.G. & DEMETS, C. (1989) Present-day motion along the Owen fracture zone and Dalrymple trough in the Arabian Sea. *J. Geophys. Res.*, **94**, 5560–5570.

GUNNELL, Y., CARTER, A., PETIT, C. & FOURNIER, M. (2007) Post-rift seaward downwarping at passive margins: new insights from southern Oman using stratigraphy to constrain apatite fission-track and (U-Th)/He dating. *Geology*, **35**, 647–650, doi:10.1130/G23639A.1.

HEY, R.N. (1977) A new class of pseudofaults and their bearing on plate tectonics: a propagating rift model. *Earth Planet. Sci. Lett.*, **37**, 321–325.

HONSHO, C., TAMAKI, K. & FUJIMOTO, H. (1996) Three-dimensional magnetic and gravity studies of the rodriguez Triple Junction in the Indian Ocean. *J. Geophys. Res.*, **101**, 15837–15848.

HUCHON, P. & KHANBARI, K. (2003) Rotation of the syn-rift stress field of the northern Gulf of Aden margin, Yemen. *Tectonophysics*, **364**, 147–166.

ILDEFONSE, B., BLACKMAN, D.K., JOHN, B.E., OHARA, Y., MILLER, D.J. & MACLEOD, C.J. INTEGRATED OCEAN DRILLING PROGRAM EXPEDITIONS 304/305 SCIENCE PARTY. (2007) Oceanic core complexes and crustal accretion at slow-spreading ridges. *Geology*, **35**, 623–626, doi:10.1130/G23531A.1.

JESTIN, F., HUCHON, P. & GAULIER, J.M. (1994) The Somalia plate and the East African rift system: present-day kinematics. *Geophys. J. Int.*, **116**, 637–654.

KLEIN, E.M., SMITH, D.K., WILLIAMS, C.M. & SCHOUTEN, H. (2005) Counter-rotating microplates at the Galapagos Triple Junction. *Nature*, **433**, 855–858.

KLEINROCK, M.C. & HEY, R.N. (1989) Detailed tectonics near the tip of the Galapagos 95.5°W propagator: how the lithosphere tears and a spreading axis develops. *J. Geophys. Res.*, **94**, 13801–13838.

KREEMER, C., HOLT, W.E. & HAINES, A.J. (2003) An integrated global model of present-day plate motions and plate boundary deformation. *Geophys. J. Int.*, **154**, 8–34.

KRUSE, S.E., TEBBENS, S.F., NAAR, D.F., LOU, Q. & BIRD, R.T. (2000) Comparisons of gravity anomalies at pseudofaults, fracture zones, and nontransform discontinuities from fast to slow spreading areas. *J. Geophys. Res.*, **105**, 28399–28410.

LAFOY, Y., AUZENDE, J.M., RUELLAN, E., HUCHON, P. & HONZA, E. (1990) The 16°40′S Triple Junction in the North Fiji Basin (SW Pacific). *Mar. Geophys. Res.*, **12**, 285–296.

LARSON, R.L., SEARLE, R.C., KLEINROCK, M.C., SCHOUTEN, H., BIRD, R.T., NAAR, D.F., RUSBY, R.I., HOOFT, E.E. & LASTHIOTAKIS, H. (1992) Roller-bearing tectonic evolution of the Juan Fernandez microplate. *Nature*, **356**, 571–576.

LASTRAS, G., CANALS, M., URGELES, R., DE BATIST, M., CALAFAT, A.M. & CASAMOR, J.L. (2004) Characterisation of the resent BIG'95 debris flow deposit on the Ebro margin, Western Mediterranean Sea, after a variety of seismic reflection data. *Marine Geology*, **213**, 235–255.

LAUGHTON, A.S, WHITMARSH, R.B. & JONES, M.T. (1970) The evolution of the Gulf of Aden. *Philos. Trans. R. Soc. London*, **A267**, 227–266.

LEPVRIER, C., FOURNIER, M., BÉRARD, T. & ROGER, J. (2002) Cenozoic extension in coastal Dhofar (southern Oman): implications on the oblique rifting of the Gulf of Aden. *Tectonophysics*, **357**, 279–293.

LEROY, S., GENTE, P., FOURNIER, M., d'ACREMONT, E., BELLAHSEN, N., BESLIER, M.-O., PATRIAT, P., MAIA, M., BLAIS, A., PERROT, J., AL-KATHIRI, A., MERKOURIEV, S., RUELLAN, P.-Y., FLEURY, J.-M., LEPVRIER, C. & HUCHON, P. (2004) From rifting to spreading in the eastern Gulf of Aden: a geophysical survey of a young oceanic basin from margin to margin. *Terra Nova*, **16**, 185–192.

LIGI, M., BONATTI, E., BORTOLUZZI, G., CARRARA, G., FABRETTI, P., GILOD, D., PEYVE, A.A., SKOLOTNEV, S. & TURKO, N. (1999) Bouvet Triple Junction in the South Atlantic: geology and evolution. *J. Geophys. Res.*, **104**, 29365–29385.

LIGI, M., BONATTI, E., BORTOLUZZI, G., CARRARA, G., FABRETTI, P., PENITENTI, D., GILOD, D., PEYVE, A.A., SKOLOTNEV, S. & TURKO, N. (1997) Death and transfiguration of a Triple Junction in the South Atlantic. *Science*, **276**, 243–245.

LONSDALE, P. (1988) Structural pattern of the Galapagos microplate and evolution of the Galapagos Triple Junction. *J. Geophys. Res.*, **93**, 13551–13574.

LUIS, J.F., MIRANDA, J.M., GALDEANO, A., PATRIAT, P., ROSSIGNOL, J.C. & MENDES VICTOR, L.A. (1994) The Azores Triple Junction evolution since 10 Ma from an aeromagnetic survey of the Mid-Atlantic Ridge. *Earth Planet. Sci. Lett.*, **125**, 439–459.

MACDONALD, K.C., FOX, P.J., PERRAM, L.J., EISEN, M.F., HAYMON, R.M., MILLER, S.P., CARBOTTE, S.M., CORMIER, M.H. & SHOR, A.N. (1988) A new view of the mid-ocean ridge from the behaviour of ridge axis discontinuities. *Nature*, **335**, 217–225.

MATTHEWS, D.H. (1966) The Owen fracture zone and the northern end of the Carlsberg Ridge. *Phil. Trans. Roy. Soc. A*, **259**, 172–186.

MATTHEWS, D.H., WILLIAMS, C. & LAUGHTON, A.S. (1967) Mid-ocean ridge in the mouth of the Gulf of Aden. *Nature*, **215**, 1052–1053.

McKENZIE, D.P. & SCLATER, J.G. (1971) The evolution of the Indian Ocean since the late cretaceous. *Geophys. J. Roy. Astronom. Soc.*, **25**, 437–528.

McKENZIE, D.P. & MORGAN, W.J. (1969) Evolution of Triple Junctions. *Nature*, **224**, 125–133.

MERKOURIEV, S. & DEMETS, C. (2006) Constraints on Indian plate motion since 20 Ma from dense Russian magnetic data: implications for Indian plate dynamics. *Geochem. Geophys. Geosyst.*, **7**, Q02002, doi:10.1029/2005GC001079.

MERCURIEV, S., PATRIAT, P. & SOCHEVANOVA, N. (1996) Evolution de la dorsale de Carlsberg: évidence pour une phase d'expansion très lente entre 40 et 25 Ma (A18 à A7). *Oceanologica Acta*, **19**, 1–13.

MINSHULL, T.A., WHITE, R.S., BARTON, P.J. & COLLIER, J.S. (1992) Deformation at plate boundaries around the Gulf of Oman. *Mar. Geol.*, **104**, 265–277.

MITCHELL, N.C. (1991) Distributed extension at the Indian Ocean Triple Junction. *J. Geophys. Res.*, **96**, 8019–8043.

MITCHELL, N.C. & LIVERMORE, R.A. (1998) The present configuration of the Bouvet Triple Junction. *Geology*, **26**, 267–270.

MITCHELL, N.C., LIVERMORE, R.A., FABRETTI, P. & CARRARA, G. (2000) The Bouvet Triple Junction, 20 to 10 Ma, and extensive transtensional deformation adjacent to the Bouvet and Conrad transforms. *J. Geophys. Res.*, **105**, 8279–8296.

MITCHELL, N.C. & PARSON, L.M. (1993) The tectonic evolution of the Indian Ocean Triple Junction, Anomaly 6 to present. *J. Geophys. Res.*, **98**, 1793–1812.

MOUNTAIN, G.S. & PRELL, W.L. (1990) A multiphase plate tectonic history of the southeast continental margin of Oman. In: *The Geology and Tectonics of the Oman Region* (Ed. by A.H.F. Robertson, M.P. Searle & A.C. Ries), *Geol. Soc. London Spec. Pub.*, **49**, 725–743.

MUNSCHY, M. & SCHLICH, R. (1989) The Rodriguez Triple Junction (Indian Ocean) – structure and evolution for the past one million years. *Mar. Geophys. Res.*, **11**, 1–14.

NOCQUET, J.-M., WILLIS, P. & GARCIA, S. (2006) Plate kinematics of Nubia–Somalia using a combined DORIS and GPS solution. *J. Geodesy*, **80**, 591–607.

NORTON, I.O. & SCLATER, J.G. (1979) A model for the evolution of the Indian Ocean and the breakup of the Gondwanaland. *J. Geophys. Res.*, **84**, 6803–6830.

OHARA, Y., YOSHIDA, T., KATO, Y. & KASUGA, S. (2001) Giant megamullion in the Parece Vela backarc basin. *Mar. Geophys. Res.*, **22**, 47–61.

PATRIAT, P. & COURTILLOT, V. (1984) On the stability of Triple Junctions and its relation to episodicity in spreading. *Tectonics*, **3**, 317–332.

PATRIAT, P. & PARSON, L. (1989) A survey of the Indian Ocean Triple Junction trace within the Antarctic plate: implications for the junction evolution since 15 Ma. *Mar. Geophys. Res.*, **11**, 89–100.

PETERS, T. & MERCOLLI, I. (1998) Extremely thin oceanic crust in the Proto-Indian Ocean: evidence from the Masirah Ophiolite, Sultanate of Oman. *J. Geophys. Res.*, **103**, 677–689.

PETIT, C., FOURNIER, M. & GUNNELL, Y. (2007) Tectonic and climatic controls on rift escarpments: erosion and flexural rebound of the Dhofar passive margin (Gulf of Aden, Oman). *J. Geophys. Res.*, **112**, B03406, doi:10.1029/2006JB004554.

QUITTMEYER, R.C. & KAFKA, A.L. (1984) Constraints on plate motions in southern Pakistan and the northern Arabian Sea from the focal mechanisms of small earthquakes. *J. Geophys. Res.*, **89**, 2444–2458.

REILINGER, R., McCLUSKY, S., VERNANT, P., LAWRENCE, S., ERGINTAV, S., CAKMAK, R., OZENER, H., KADIROV, F., GULIEV, I., STEPANYAN, R., NADARIYA, M., HAHUBIA, G., MAHMOUD, S., SAKR, K., ARRAJEHI, A., DEMITRIS, S., AL-AYDRUS, A., PRILEPIN, M., GUSEVA, T., EVREN, E., DMITROTSA, A., FILIKOV, S.V., GOMEZ, F., AL-GHAZZI, R. & KARAM, G. (2006) GPS constraints on continental deformation in the Africa–Arabia–Eurasia continental collision zone and implications for the dynamics of plate interactions. *J. Geophys. Res.*, **111**, B05411, doi:10.1029/2005JB004051.

ROYER, J.-Y., CHAUBEY, A.K., DYMENT, J., BHATTACHARYA, G.C., SRINIVAS, K., YATHEESH, V. & RAMPRASAD, T. (2002) Paleogene plate tectonic evolution of the Arabian and Eastern Somali basins. In: *The Tectonic & Climatic Evolution of the Arabian Sea Region* (Ed. by P. Clift, D. Kroon, C. Gaedicke & J. Craig), *Geol. Soc. Spec. Publ.*, **195**, 7–23.

SAHOTA, G. (1990) Geophysical investigations of the Gulf of Aden Continental Margins: Geodynamic implications for the Development of the Afro-Arabian Rift System, PhD Thesis, University College, Swansea.

SCHMIDT, J. (1932) *Dana's Togt Omkring Jorden, 1928–1930*, Gyldendal edn. Copenhagen, 269pp.

SCLATER, J.G., BOWIN, C., HEY, R., HOSKINS, H., PEIRCE, J., PHILLIPS, J. & TAPSCOTT, C. (1976) The Bouvet Triple Junction. *J. Geophys. Res.*, **81**, 1857–1869.

SEARLE, R. (1980) Tectonic pattern of the Azores spreading center and Triple Junction. *Earth Planet. Sci. Lett.*, **51**, 415–434.

SEARLE, R., CANNAT, M., FUJIOKA, K., MÉVEL, C., FUJIMOTO, H., BRALEE, A. & PARSON, L. (2003) Fuji Dome: a large detachment fault near 64°E on the very slow-spreading southwest Indian Ridge. *Geochem. Geophys. Geosyst.*, **4**, 9105, doi:10.1029/2003GC000519.

SELLA, G.F., DIXON, T.H. & MAO, A.L. (2002) REVEL: a model for Recent plate velocities from space geodesy. *J. Geophys. Res.*, **104**, doi:10.1029/2000JB000033.

SHILLINGTON, D.J., HOLBROOK, W.S., VAN AVENDONK, H.J.A., TUCHOLKE, B.E., HOPPER, J.R., LOUDEN, K.E., LARSEN, H.C. & NUNES G, .T. (2006) Evidence for asymmetric nonvolcanic rifting and slow incipient oceanic accretion from seismic reflection data on the Newfoundland margin. *J. Geophys. Res.*, **111**, B09402, doi:10.1029/2005JB003981.

SMEWING, J.D., ABBOTTS, I.L., DUNNE, L.A. & REX, D.C. (1991) Formation and emplacement ages of the Masirah ophiolite, Sultanate of Oman. *Geology*, **19**, 453–456.

SPENCER, S., SMITH, D.K., CANN, J.R., LIN, J. & MCALLISTER, E. (1997) Structure and stability of non-transform discontinuities on the Mid-Atlantic Ridge between 24°N and 30°N. *Mar. Geophys. Res.*, **19**, 339–362.

SRIVASTAVA, S.P., SCHOUTEN, H., ROEST, W.R., KLITGORD, K.D., KOVACS, L.C., VERHOEF, J. & MACNAB, R. (1990) Iberian plate kinematics: a jumping plate boundary between Eurasia and Africa. *Nature*, **344**, 756–759.

STEIN, C.A. & COCHRAN, J.R. (1985) The transition between the Sheba ridge and the Owen basin: rifting of old oceanic lithosphere. *Geophys. J. Roy. Astronom. Soc.*, **81**, 47–74.

SYKES, L.R. (1968) Seismological evidence for transform faults, sea floor spreading, and continental drift. In *History of the Earth's Crust, A Symposium* R.A Phinney), pp. 120–150. Princeton University Press, Princeton.

SYKES, L.R. (1970) Earthquake swarms and sea-floor spreading. *J. Geophys. Res.*, **75**, 6598–6611.

TALLING, P.J., WYNN, R.B., MASSON, D.G., FRENZ, M., CRONIN, B.T., SCHIEBEL, R., AKHMETZHANOV, A.M., DALLMEIER-TIESSEN, S., BENETTI, S., WEAVER, P.P.E., GEORGIOPOULOU, A., ZÜHLSDORFF, C. & AMY, L.A. (2007) Onset of submarine debris flow deposition far from original giant landside. *Nature*, **450**, 541–544, doi:10.1038/nature06313.

TAPSCOTT, C.R., PATRIAT, P., FISHER, R.L., SCLATER, J.G., HOSKINS, H. & PARSONS, B. (1980) The Indian Ocean Triple Junction. *J. Geophys. Res.*, **85**, 4723–4739.

TIBERI, C., LEROY, S., D'ACREMONT, E., BELLAHSEN, N., EBINGER, C., AL-LAZKI, A. & POINTU, A. (2007) Crustal geometry of the northeastern Gulf of Aden passive margin: localization of the deformation inferred from receiver function analysis. *Geophys. J. Int.*, **168**, 1247–1260.

TUCHOLKE, B.E., LIN, J. & KLEINROCK, M.C. (1998) Megamullions and mullion structure defining oceanic metamorphic core complexes on the Mid-Atlantic Ridge. *J. Geophys. Res.*, **103**, 9857–9866.

VAN WIJK, J.W. & BLACKMAN, D.K. (2005) Deformation of oceanic lithosphere near slow-spreading ridge discontinuities. *Tectonophysics*, **407**, 221–225.

VIGNY, C., HUCHON, P., RUEGG, J.C., KHANBARI, K. & ASFAW, L.M. (2006) Confirmation of Arabia plate slow motion by new GPS data in Yemen. *J. Geophys. Res.*, **111**, B02402, doi:10.1029/2004JB003229.

VOGT, P.R. & JUNG, W.Y. (2004) The Terceira Rift as hyper-slow, hotspot-dominated oblique spreading axis: a comparison with other slow-spreading plate boundaries. *Earth Planet. Sci. Lett.*, **218**, 77–90.

WESSEL, P.W. & SMITH, M.F. (1991) Free software helps map and display data. *EOS Trans. AGU*, **72**, 441–446.

WHITMARSH, R.B. (1979) The Owen Basin off the South-East margin of Arabia and the evolution of the Owen Fracture Zone. *Geophys. J. Roy Astronom. Soc.*, **58**, 441–470.

WHITMARSH, R.B., WESER, O.E., ROSS, D.A., & DSDP LEG 23 SHIPBOARD SCIENTIFIC PARTY. (1974) Initial report DSDP, US Government Printing Office, Washington, DC, Vol. 23, p. 1180.

WILSON, T.J. (1965) A new class of faults and their bearing on continental drift. *Nature*, **207**, 343–347.